

## Supplementary information

# Facile preparation of siloxane-capped amorphous nano- $\text{SiO}_x$ /graphite with improved dispersion ability and battery anode performance

Jong-Seon Kim, Cao Cuong Nguyen, Hyun-Jin Kim, and Seung-Wan Song\*

*Department of Fine Chemical Engineering & Applied Chemistry, Chungnam  
National University, Daejeon, 305-764, Republic of Korea*

E-mail: swsong@cnu.ac.kr

### Experimental

**Synthesis of siloxane-capped amorphous  $\text{SiO}_x$  nanoparticles:** silicon tetrachloride ( $\text{SiCl}_4$ , 99 %, Aldrich), 1,2-dimethoxyethane (Glyme, 99.5 %, Aldrich) and methoxytrimethylsilane (MTMS, 99 %, Aldrich) and lithium powder (20 - 30  $\mu\text{m}$ , SLMP<sup>®</sup>, FMC) were used as received. 0.216 mole of  $\text{SiCl}_4$  together with 0.648 mole of MTMS were added to 500 ml of glyme solvent under stirring at room temperature in the argon-filled glove box (MOTek) with water and oxygen contents of 1 ppm. The mixed solution in the tightly closed bottle was sonicated for 2 h in a sonicator (JEIOTECH, UC-05) at 40kHz. Then, 0.864 mole of lithium powder was added to the mixed solution. The bottle was tightly closed and moved out to ultrasonic bath and was sonicated for 2h at room temperature, followed by magnetic stirring for 16h. The formation of dark powders was observed. Resultant powders were separated from glyme and MTMS by centrifugation. 1M HCl in the mixed solution of acetone and deionized water (2:1 volume ratio)

was added to the resultant powders while being sonicated, in order to remove residual lithium powder by converting lithium metal to lithium chloride (LiCl) that are soluble in aqueous solution. Note that washing with water-containing solution to remove LiCl could cause hydrolysis of some siloxane, increasing oxygen content in  $\text{SiO}_x$ . Separation of powder from the mixed solution by centrifugation and washing them with acetone-water mixed solution were repeated several times till the complete removal of lithium chloride, while checking the presence of chloride anion in the solution as the formation of white silver chloride ( $\text{AgCl}$ ) precipitates using silver nitrate ( $\text{AgNO}_3$ ) solution. After drying the resultant powders in vacuum oven at  $30^\circ\text{C}$  overnight, dark grey siloxane-capped amorphous  $\text{SiO}_x$  nanoparticles (Figure S1) were obtained.

**Material characterization:** the presence of both silicon and oxygen and their relative atomic ratio of the synthesized siloxane-capped amorphous  $\text{SiO}_{0.26}$  nanoparticles were determined by transmission electron microscopy-energy dispersive X-ray (TEM-EDX, JEOL JEM-2100F) spectral analysis. Relative atomic ratio of Si to O is 87:13 wt%. Considering that the detection limit of HRTEM elemental mapping in our measurement condition is in the range of 0.5 - 3 wt%, the chemical formula to  $\text{SiO}_{0.26\pm 0.02}$  was determined. Carbon content of trimethyl groups from siloxane was confirmed with automatic elemental analyzer (Thermo Fisher Scientific, Flash EA1112). Crystal structure was determined by X-ray diffraction analysis using powder X-ray diffractometer (Bruker AXS/D8 Discover) with Ni-filtered  $\text{Cu K}\alpha$  radiation at 40 kV and 40 mA, which was measured in  $10 - 80^\circ 2\theta$  with the scan rate of  $2^\circ/\text{min}$  at  $0.05^\circ$  step. The presence of self-organized siloxanes formed at the surface of  $\text{SiO}_x$  nanoparticles was examined using attenuated total reflection (ATR) IR spectrometer (Nicolet 670) equipped with Ge optic and mercury-cadmium-telluride (MCT) detector, under dry nitrogen. IR spectra were collected with 512 scans and spectral resolution of  $4\text{ cm}^{-1}$ . For the determination of particle size and morphology, high-resolution (HR) TEM analysis was conducted at 200 kV. Particle morphology was also examined using field-emission scanning electron microscopy (FE SEM, Sirion) at 10 kV. Surface area was determined by  $\text{N}_2$  adsorption at  $-196^\circ\text{C}$  using adsorption apparatus (Belsorp-max) and Brunauer-Emmett-Teller (BET) equation. The relative elemental distribution of carbon and silicon of the  $\text{SiO}_{0.26}/\text{graphite}$  composite electrode was examined using FE SEM-EDX.

**Electrochemical characterization:** The electrode of  $\text{SiO}_{0.26}$  was prepared by casting a slurry, which consisted of 50 wt% siloxane-capped amorphous nano- $\text{SiO}_{0.26}$  active material, 35 wt% carbon black (super-P), and 15 wt% polyacrylic acid (PAA, MW 450,000 Aldrich) in N-methylpyrrolidinone (NMP), on a 13  $\mu\text{m}$  thick copper foil. The coated electrode was dried in a vacuum oven at 30 °C for 12h and at 110 °C overnight. The 2016 coin half-cells, which consist of siloxane-capped amorphous nano- $\text{SiO}_{0.26}$  electrode as a working electrode, a lithium counter electrode, separator (Celgard C210) and the electrolyte of 1M  $\text{LiPF}_6$ /fluoroethylene carbonate (FEC) : diethyl carbonate (DEC) (1:1 volume ratio, PanaX e-tec) with 3 wt% trimethyl phosphite ( $\text{P}(\text{OCH}_3)_3$ , 99 %, Aldrich) as an acid (e.g.,  $\text{PF}_5$ ,  $\text{PF}_3\text{O}$ )-scavenging additive, were assembled in argon-filled glove box for testing of electrochemical charge–cycling ability. The lithium coin-cells were cycled in constant current (CC)-constant voltage (CV) mode in the voltage region of 0.01 - 1.5 V using a multichannel cycler (Won-A Tech). Constant current (CC) of  $300 \text{ mA g}^{-1}$  (corresponding to  $\sim 0.12\text{C}$ ,  $1\text{C} = 2.5 \text{ A/g}$ ) was applied till 0.01 V followed by holding the voltage at 0.01 V till the current flowed is lower than  $100 \text{ mA g}^{-1}$ . For testing of rate capability, after the first cycle at the rate of 0.12C, the lithium cell was charged at various C-rates of 0.24C ( $600 \text{ mA g}^{-1}$ ), 0.6C ( $1.5 \text{ A g}^{-1}$ ), 1.2C ( $3 \text{ A g}^{-1}$ ), 3.6C ( $9 \text{ A g}^{-1}$ ) and 6C ( $15 \text{ A g}^{-1}$ ), and discharged at the fixed rate of 0.12C. Cycling ability in the conventional electrolyte of 1M  $\text{LiPF}_6$ /ethylene carbonate (EC) : ethylmethyl carbonate (EMC) (3:7 volume ratio, Soulbrain) and silicon oxide ( $\text{SiO}_{1.24}$ ) nanoparticles synthesized in the absence of surface siloxane-capping in the electrolyte of 1M  $\text{LiPF}_6$ /FEC:DEC (5:5 volume ratio) with 3wt% trimethyl phosphite additive was tested for comparison. AC impedance spectral measurement was conducted for siloxane-capped  $\text{SiO}_{0.26}$  and bare  $\text{SiO}_{1.24}$  electrodes at OCV and after the 1<sup>st</sup> cycle in 1M  $\text{LiPF}_6$ /FEC:DEC with 3wt% trimethyl phosphite, using an impedance analyzer (VSP SP-150, Bio-Logic) in the frequency range of 400kHz to 10 mHz with an amplitude of 10 mV.

For the preparation of  $\text{SiO}_{0.26}$ /graphite composite electrode, siloxane-capped amorphous nano- $\text{SiO}_{0.26}$  and carbon black powders were first mixed by grinding for 30min, mixed with the binder solution of 3wt% PAA in NMP and was sonicated for 10min in a sonicator. Graphite powders (Aldrich, 20  $\mu\text{m}$ ) were added to the mixture solution and sonicated for 10min, and the slurry was prepared. The  $\text{SiO}_{0.26}$ /graphite composite electrode, which consists of 70 wt% of  $\text{SiO}_{0.26}$  and graphite (35:35 wt%) active material, 15 wt% carbon black (super-P), and 15 wt%

PAA binder, was coated on a copper foil and vacuum-dried at 30 °C for 12h and at 110 °C overnight. The 2016 coin half-cells, which consist of  $\text{SiO}_{0.26}$ /graphite electrode as a working electrode, a lithium counter electrode, separator (Celgard C210) and the electrolyte of 1M  $\text{LiPF}_6/\text{FEC}:\text{DEC}$  with 3 wt% trimethyl phosphite, were assembled in argon-filled glove. Coin-cells were cycled in a constant current (CC) at  $300 \text{ mA g}^{-1}$  ( $\sim 0.3\text{C}$ )-constant voltage (CV) mode in the voltage region of 0.01 - 1.5 V.

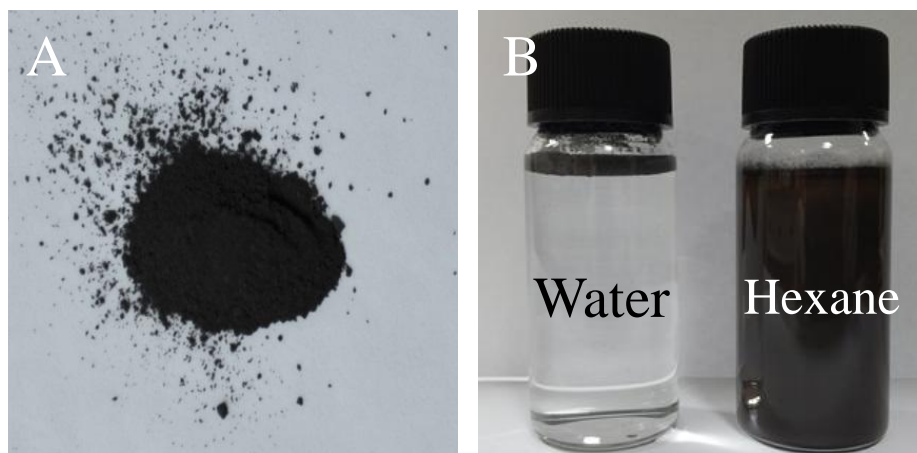


**Figure S1.** (A) As-synthesized siloxane-capped amorphous  $\text{SiO}_{0.26}$  nanoparticles and (B) their dispersion ability in water and hexane, respectively.

Synthesized siloxane-capped amorphous  $\text{SiO}_{0.26}$  nanoparticles were dark grey (Figure S1A). Surface capping with trimethyl-terminated siloxane molecular linkages results in hydrophobic nature of particle surface, which is highly effective in dispersing in organic solvents such as hexane (Figure S1B) and acetone (Figure 2A), whereas the particles were not wet in water as shown in Figure S1B. Such high dispersion ability is advantageous for homogeneous dispersion of our siloxane-capped amorphous  $\text{SiO}_{0.26}$  nanoparticles with carbon powders in NMP when preparing carbon composites, and also facile wetting in carbonate-based organic electrolytes. Homogeneous distribution of constituents is expected to provide homogeneous current distribution over the composite electrode and superior cycling performance to those prepared just by a physical mixing.

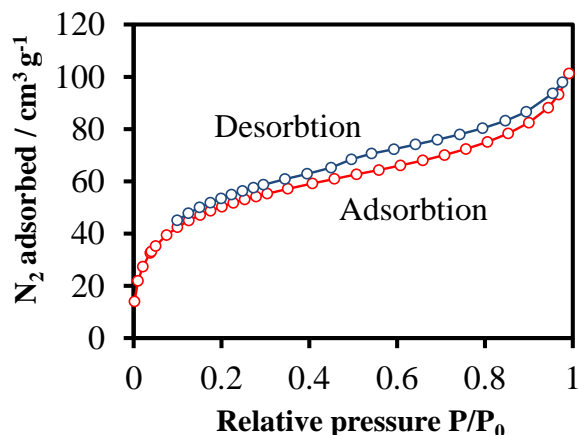


**Figure S2.** N<sub>2</sub> adsorption-desorption isotherm of siloxane-capped amorphous SiO<sub>0.26</sub> nanoparticles .

N<sub>2</sub> adsorption-desorption isotherm behavior of the siloxane-capped amorphous SiO<sub>0.26</sub> nanoparticles shows a clear condensation step at relative pressure and a hysteresis loop, identified as type H4.<sup>1</sup> This is characteristic of slit-shaped pores, as in many activated carbon. Pore size distribution is mainly in the micropore range. The H4-type loops do not close until the equilibrium pressure is at, or very close to, the saturation pressure.<sup>2</sup> We estimate that surface siloxane molecular linkages interrupt N<sub>2</sub> gas adsorption-desorption at the surface of SiO<sub>x</sub> nanoparticles. The micropores may exist in between siloxane-capped amorphous SiO<sub>0.26</sub> nanoparticles. The surface area determined by the Brunauer-Emmett-Teller (BET) measurement is 170 m<sup>2</sup>/g. This large surface area with the presence of micropores would be effective in releasing structural stress upon lithiation-delithiation and providing facile electrolyte wetting and ion-transport kinetics.

#### References

- (1) K. Sing, D. Everett, R. Haul, L. Moscou, R. Pierotti, J. Rouquerol, *IUPAC Recomm. Pure Appl. Chem.*, 1985, **57**, 603.
- (2) F. Rouquerol, J. Rouquerol, K. Sing, *Adsorption by Powders & Porous Solids*; Academic Press: San Diego, 1999.

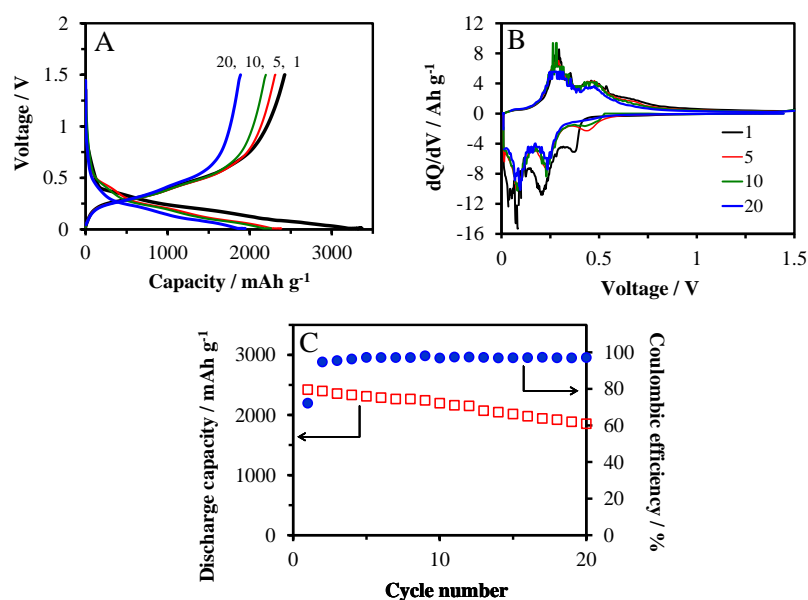


**Figure S3.** Cycling ability of siloxane-capped amorphous nano-SiO<sub>0.26</sub> electrode at 0.12C in 1M LiPF<sub>6</sub>/EC:EMC; (A) voltage profiles, and plots of (B) differential capacity and (C) discharge capacity and coulombic efficiency over 20 cycles.

In the conventional electrolyte of 1M LiPF<sub>6</sub>/EC:EMC, the electrode at the rate of 0.12C delivers 2422–1853 mAhg<sup>-1</sup> with the capacity retention of 76% at the 20th cycle and coulombic efficiencies of 96-98 %. Although the resultant capacity value and retention are still greater than previously reported SiO or SiO<sub>x</sub><sup>18,19</sup> bulk electrodes probably due to our interfacial stabilized artificial SEI-capped SiO<sub>0.26</sub>, the performance is inferior to those in FEC-based electrolyte (Figure 2). Cycling ability of SiO<sub>x</sub> electrode enables to be further improved when choosing suitable electrolyte component with higher interfacial compatibility with the electrode.

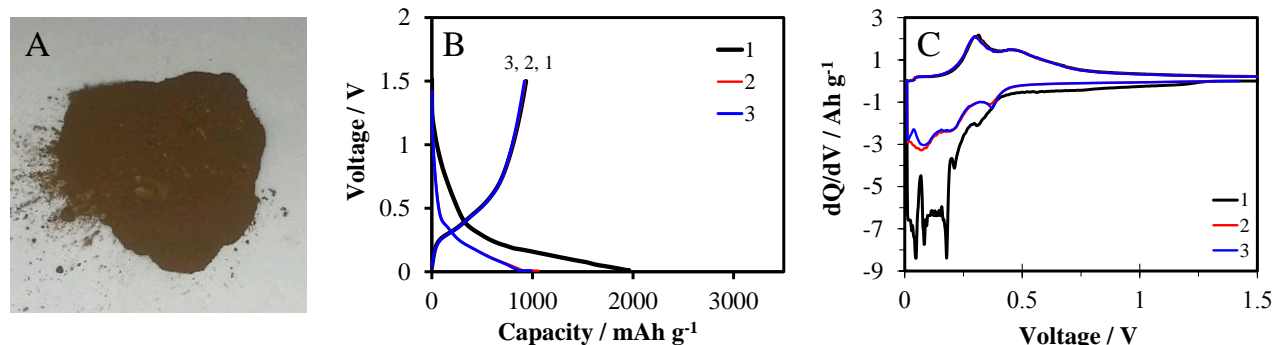


**Figure S4.** (A) Silicon oxide ( $\text{SiO}_{1.24}$ ) nanoparticles synthesized in the absence of surface siloxane-capping, and (B) voltage profiles and (C) differential capacity plots of the lithium cell with  $\text{SiO}_{1.24}$  electrode at 0.12C in 1M  $\text{LiPF}_6/\text{FEC}:\text{DEC}$  with 3wt% trimethyl phosphite additive.

In the absence of surface siloxane-capping by synthesizing without the use of MTMS (methoxytrimethylsilane), silicon oxide nanoparticles with higher fraction of oxygen ( $\text{SiO}_{1.24}$ ) were synthesized. Obtained  $\text{SiO}_{1.24}$  nanoparticles are brown (Figure S4A) and brighter than siloxane-capped  $\text{SiO}_{0.26}$  nanoparticles (Figure S1). Brighter color is due to higher oxygen content than  $\text{SiO}_{0.26}$ . This imposes that the role of MTMS is to protect  $\text{SiO}_{0.26}$  nanoparticles against further oxidization during synthesis. Figure S4B shows voltage profiles for three cycles of  $\text{SiO}_{1.24}$  electrode in the voltage region of 0.01 - 1.5 V in a constant current of  $300 \text{ mA g}^{-1}$  (0.12C)–constant voltage mode. Initial charge and discharge capacities are 2246 and  $936 \text{ mAh g}^{-1}$ , respectively, corresponding to a very low initial coulombic efficiency of 41%. The low efficiency is due to irreversible formation of a plenty of  $\text{Li}_2\text{O}$  and lithium silicates, as observed in differential capacity plots (Figure S4C) as a large irreversible capacity loss after the first lithiation. Large oxygen content of  $\text{SiO}_{1.24}$  electrode might reduce the discharge capacity.

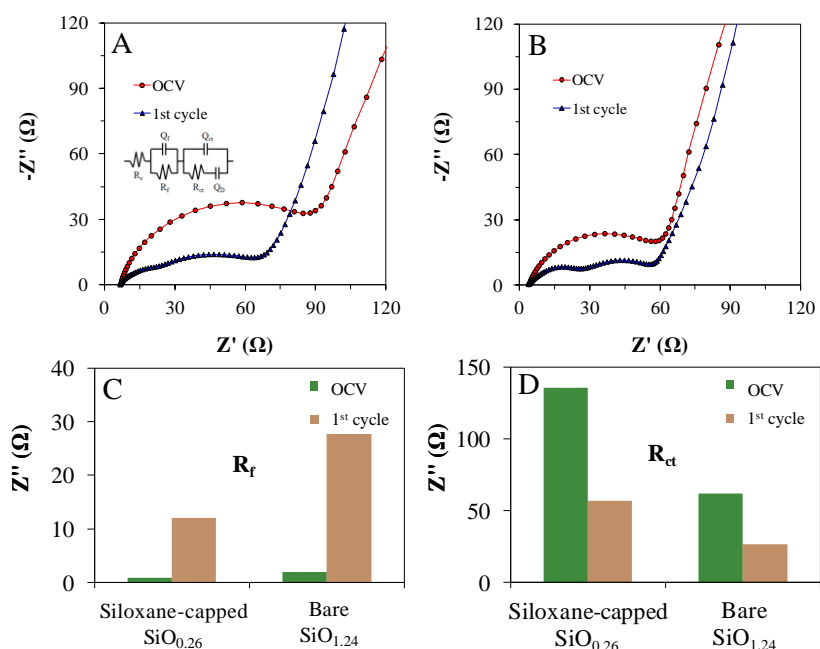
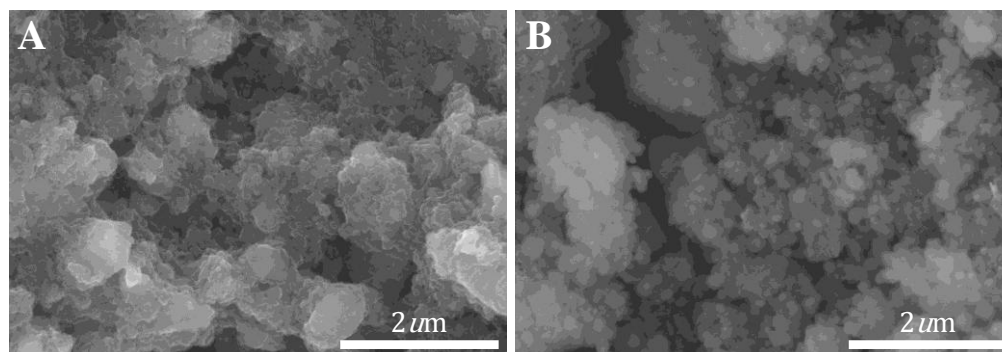


Figure S5. Impedance spectral comparison for the electrodes of (A) siloxane-capped  $\text{SiO}_{0.26}$  and (B) bare  $\text{SiO}_{1.24}$  at open-circuit voltage (OCV) and after the 1<sup>st</sup> cycle in 1M  $\text{LiPF}_6/\text{FEC}:\text{DEC}$  with 3wt% trimethyl phosphate, and interfacial resistances of  $R_f$  and  $R_{ct}$  obtained by curve-fitting the spectra using an equivalent circuit model displayed in the inset.

Electrochemical AC impedance spectral data provide the effect of siloxane-capping on interfacial resistance. All spectra (Fig. S5 A-B) consist of semicircles in a high frequency range associated with film resistance of the SEI layer ( $R_f$ ) due to migration of the  $\text{Li}^+$  ions through the surface film and the medium-to-low frequency one with charge transfer resistance ( $R_{ct}$ ) at the electrode-electrolyte interface. Those interfacial resistances were determined by fitting the spectra using the equivalent circuit model (inset in Fig. S5A) and summarized in Fig. S5C-D. At OCV, siloxane-capped  $\text{SiO}_{0.26}$  electrode exhibits much larger  $R_{ct}$  than less electronically conductive bare  $\text{SiO}_{1.24}$ , which is due to the presence of non-conductive siloxanes at the surface of  $\text{SiO}_{0.26}$  electrode. Nonetheless, after the 1<sup>st</sup> cycle, siloxane-capped of  $\text{SiO}_{0.26}$  undergoes a substantial decrease in the  $R_{ct}$ , probably due to the formation of a stable SEI layer. Since the siloxanes could prevent a direct contact between  $\text{SiO}_{0.26}$  and electrolyte, it can reduce the degree of electrolyte decomposition. That is why relatively smaller change is there in the  $R_f$ , in contrast to significant increase in  $R_f$  for  $\text{SiO}_{1.24}$  electrode that has no surface-protective layer.



**Figure S6.** Comparison of SEM images of siloxane-capped amorphous nano-SiO<sub>0.26</sub> (A) pristine electrode (A) and (B) the electrode after 50 cycles in 1M LiPF<sub>6</sub>/FEC:DEC with 3wt% trimethyl phosphite additive.

Figure S5 exhibits particle morphology change of the electrode before and after cycling. For pristine electrode (Figure S5A), nanoparticles are in a vague shape and seem to be aggregated. After cycling (Figure S5B), particle shape becomes clearly spherical and relatively less aggregated. Enlargement of particle size or particle cracking, which was usually observed on cycled Si-based anodes, are not observed in our electrode, implying an accommodation of volume change. Formation of new dissimilar particles of the SEI components is also not noticeable, by a successful surface protection by siloxane capping.

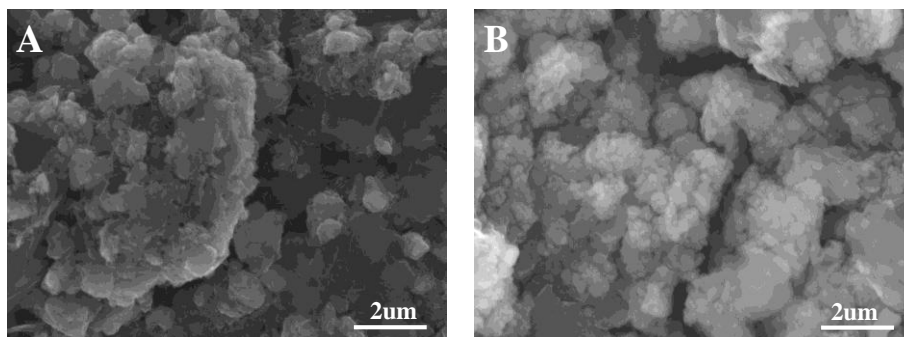


**Figure S7.** Comparison of SEM images of SiO<sub>0.26</sub>/graphite electrodes of (A) pristine and (B) after 100 cycles in 1M LiPF<sub>6</sub>/FEC:DEC with 3wt% trimethyl phosphite additive.

Pristine electrode (Figure S6A) shows well mixed SiO<sub>0.26</sub> nanoparticles and graphite micron powders. After cycling (Figure S6B), neither particle cracking nor aggregation is observed. The presence of graphite, homogeneous distribution of artificial SEI-capped amorphous nano-SiO<sub>0.26</sub> and graphite, the use of interfacially compatible electrolyte appear to provide microstructural robustness of composite electrode.